In-flow detection of ultra-small magnetic particles by an integrated giant magnetic impedance sensor

Kamel Fodil, Matthieu Denoual, Christophe Dolabdjian, A. Treizebre, Vincent Senez

In-flow detection of ultra-small magnetic particles by an integrated giant magnetic impedance sensor

Cite as: Appl. Phys. Lett. **108**, 173701 (2016); https://doi.org/10.1063/1.4948286
Submitted: 25 February 2016 • Accepted: 15 April 2016 • Published Online: 27 April 2016

K. Fodil, M. Denoual, C. Dolabdjian, et al.

In-flow detection of ultra-small magnetic particles by an integrated giant magnetic impedance sensor

K. Fodil,[1] M. Denoual,[2,a)] C. Dolabdjian,[1] A. Treizebre,[3] and V. Senez[3,a)]
[1]*Normandie Univ, CNRS, UMR 6072 - GREYC, Caen 14000, France*
[2]*École Nationale Supérieure d'Ingénieurs de Caen, UMR 6072 - GREYC, Caen F-14000, France*
[3]*Univ. Lille, CNRS, ISEN, UMR 8520 - IEMN, Lille F-59000, France*

(Received 25 February 2016; accepted 15 April 2016; published online 27 April 2016)

We have designed and fabricated a microfluidic system made of glass and polydimethylsiloxane. A micro-magnetometer has been integrated to the system. This sensor is made of a giant magneto-impedance wire known to have very high magnetic sensitivity at room temperature. A liquid-liquid segmented multiphase flow was generated in the channel using a Y-shaped inlet junction. The dispersed phase plugs contained superparamagnetic iron oxide (20 nm) nanoparticles at a molar concentration of 230 mmol/l. We have shown both theoretically and experimentally that in-flow detection of these nanoparticles is performed by the microsystem for concentration as small as 5.47×10^{-9} mol. These performances show that it is conceivable to use this system for *ex-vivo* analysis of blood samples where superparamagnetic iron oxide nanoparticles, initially used as magnetic contrast agents, could be functionalized for biomarkers fishing. It opens new perspectives in the context of personalized medicine. *Published by AIP Publishing.*
[http://dx.doi.org/10.1063/1.4948286]

With the continuous innovations in biotechnologies, the "omics," biomedical imaging, computer technologies, and nanotechnologies, the concept of "personalized medicine" or theranostics where patients will benefit from a targeted therapy in accordance with their molecular profile is progressing.[1] This approach includes *in vitro* measurements performed on biological fluids, *ex vivo* analysis of biopsies and/or medical imaging to evaluate the patient's clinical status. The development of multifunctional (i.e., diagnostic, therapeutic, and imaging) nanoparticles is a key component for its future clinical implementation and nanotechnologists are looking for an ideal material that can be used at the same time for *in-vivo* and *ex-vivo* analyses.[2,3]

Magnetic nanoparticles have long been studied as contrast agents (CAs) for magnetic resonance imaging (MRI). Thanks to recent progress in synthesis and surface modification, they are now considered as potential candidates for theranostics.[4] Superparamagnetic iron oxide (SPIO) are probably the most extensively used MRI CAs.[5,6]

Their potential application in biomedicine is wide (i.e., magnetic particles imaging, controlled drug release, molecular or cellular tagging, or hyperthermia treatment), since they are safer than gadolinium and fluorine based CAs.[7,8] They can be classified into three groups: ultra-small PIO (USPIO, <50 nm), small PIO (SPIO, 50–150 nm), and micrometer-sized PIO (MPIO, >1 μm).[9] USPIO allows imaging of liver tumors, metastatic lymph nodes, inflammatory atherosclerotic plaques, functional MRI, magnetic resonance (MR) angiography, measurement of tumor microvascular permeability, cell tracking (i.e., stem cell migration), etc. Clinical benefit from these particles has moved far beyond the single proof of concept stage.[10]

Body fluid analysis assumes that the tissues liberate proteins, carbohydrates, lipids, mineral ions, hormones, cells, and/or cell components in the fluids, and that the disease change either their spectrum or their concentration.[11,12] Several platforms able to detect molecular biomarkers from body fluids have been developed.[13] Unfortunately, very few have been translated into clinical applications because they most often rely on a complex preparation of the raw sample, they can only perform testing at limited and discrete time points, they have limited access to clinically relevant anatomic sites and they suffer from the small sampling volume and induced a sampling error. This ascertainment led to the development of alternative approaches where the entire body fluid volume can be scanned by *in-vivo* flow cytometry[14,15] and/or larger sampling volume is performed for further *in-vitro* characterization by various molecular profiling techniques.[16–18] Recently, magnetic probe-based fishing coupled to microfluidics has emerged as a powerful tool for the analysis of body fluids.[19–21] Since biological species have very low magnetic susceptibility, magnetic actuation and sensing are non-invasive compared to optical, acoustic, or electrical means. The lack of magnetic background enables actuation and sensing on magnetically labeled bio-species in unprocessed body fluids without interference with non-tagged bio-species or sensitivity to physical conditions (pH, temperature, salinity, etc.).

Several types of room temperature solid state magnetometers have been designed and tested with the constraints of microsystems: giant magneto-resistive (GMR) sensors,[22–27] fluxgates,[28–30] hall sensors,[31–33] and recently giant magneto-impedance (GMI) sensors.[34–37] GMI sensors are promising, thanks to their sensitivity and noise properties.[38] Some platforms present a static detection where the magnetic nanoparticles used as labels for the bio-species are immobilized on the magnetometer.[39] This quantitative approach has two

a)Authors to whom correspondence should be addressed. Electronic addresses: matthieu.denoual@ensicaen.fr and vincent.senez@isen.fr

disadvantages. It is limited by the sensor's surface and thus by the number of immobilized species. It also requires careful selection of sample flow rate. Dynamic approach where the magnetic nanoparticles are detected while flying over the magnetometer can overcome these drawbacks. First attempts used ferrofluid droplets (microns size)[40] or single particles[41] moving inside micro-channels. Recently, this technique has been implemented for cytometer application using GMR[42–46] and GMI magnetometer.[47–49] A critical issue is to show the real-time detection at room temperature. Here, we report on the development of a microfluidic system integrating a GMI sensor for *ex-vivo* analysis of blood biomarkers endogenously or exogenously labelled with USPIO nanoparticles.

The detection of the USPIOs P03299 (20 nm diameter functionalized with polyethylene glycol, GUERBET, France.) relies on the application of an external magnetic field $\overrightarrow{H_{ext}}$ to induce their magnetization $\vec{M}$ (1).

$$\vec{M} = \chi \cdot \upsilon_t \cdot \overrightarrow{H_{ext}}, \tag{1}$$

where χ and υ_t are the magnetic susceptibility and the total volume of the USPIOs, respectively. A magnetic sensor senses the stray magnetic induction $\vec{B}$ (2) generated by the presence of magnetized USPIOs. It yields

$$\vec{B} = \frac{\mu_0}{4\pi} \overrightarrow{grad}\left(\frac{\vec{M} \cdot \vec{r}}{r^3}\right), \tag{2}$$

where μ_0 is the permeability of free space ($4\pi \times 10^{-7}$ H/m). As the magnetic susceptibility is proportional to the concentration of USPIOs (1), the magnetic induction depends on both their volume and concentration. Usually, the external, magnetic induction is perpendicular to the sensitive axis of the sensor[35,50] to prevent its saturation and to enable high dynamic range measurements (Fig. 1). The detection of the USPIOs is carried out in a fluidic microsystem which consists of a rectangular micro-channel (70 μm × 170 μm) and glass round capillaries (75 μm) for the injection of the fluid.

A thin 10/500 nm thick metal (Ti/Au) bilayer is deposited on a glass substrate, 150 μm thick, through an aluminum shadow mask by cathodic pulverization to pattern the electric pads to connect the GMI wire. The shadow mask is made of an aluminum foil machined by drilling technology. This technique is classically used when the size of the patterns is

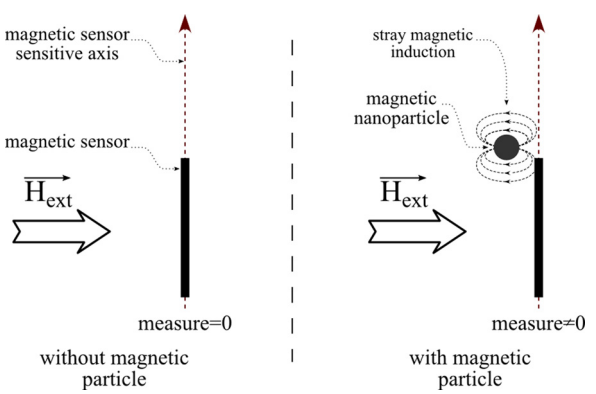

FIG. 1. Simplified sketch view of the detection principle.

in the millimeter range. The shadow mask is placed on the glass substrate and both of them are fixed on the chuck of the deposition equipment. Ti/Au layers are deposited by the bombardment of solid material target with energetic particles extracted from cold argon plasma at low pressure (250 W – 125 V – 80 sccm). The deposition process is performed during 25 s for the titanium layer and 1 min for the gold layer. The GMI microwire (10 mm long and 40 μm in diameter), made of CoFeSiBNb alloy (MXT Inc), is manually set up between the pads and bonded to the pads by conductive epoxy glue. In parallel, the polydimethylsiloxane (PDMS) microfluidic part is fabricated using replica molding. PDMS is classically used since it is easy to process, biocompatible and transparent. The material is supplied in two components, a base and a curing agents (DOW CORNING SYLGARD 184 Silicone Elastomer). Silicon hydride groups present in the curing agent react with vinyl groups present in the base and form a cross-linked elastomeric solid. The fabrication of the microfluidic network starts with the production of the master mold in the silicon substrate (Siltronix Silicon Prime wafers CZ) (diameter: 76.2 ± 0.3 mm, thickness: 380 ± 25 μm, orientation: ⟨100⟩, type doping: P-Boron, resistivity: 1–10 Ω cm). Selective etching of silicon is obtained by protection of the silicon surface with a resist mask. AZ9260 positive photo-resist (from MicroChemicals) is spin-coated to obtain a 10 μm thick layer. The spin parameters are: speed = 1500 rpm, acceleration = 3000 rpm s^{-1}, and time 40 s. The substrate is soft-baked during 90 s at 110 °C on a hotplate and AZ9260 is exposed to UV radiation at λ = 365 nm for 20 s. Exposed resist is removed by the AZ351B developer (from MicroChemicals) during 90 s and rinsed with water during 15 s. The resist-covered substrate is put in a 110 °C furnace for an hour to improve the masking efficiency during the etching process. The substrate is etched by a deep reactive ion etching (DRIE) process, with C4F8 passivation and SF6 etching steps. This technique is called "Bosh" process and is performed with an STS DRIE plasma equipment. The parameters are: C4F8 flow rate = 100 sccm; passivation time = 2.2 s; RIE/ICP power = 20 W/1500 W; SF6 flow rate = 450 sccm; etching time = 3 s; and RIE/ICP power = 50 W/2200 W. During this process, the substrate chiller is cooled down to −10 °C in order to improve the thermal evacuation. The etching rate is 5.5 μm/min and the etching depth is 150 μm corresponding to the outer diameter of the glass capillaries that are bonded to the device and connected to the fluidic pumps. After this etching step, a thin layer of "Teflon" like coating is deposited on the surface of the silicon substrate using a C4F8 plasma to make easier the peeling of PDMS. The liquid mixture containing the precursor and the curing agent (10:1 (v/v)) is poured on the silicon mold and polymerized on furnace at 80 °C during 1 h. It conforms to the shape of the mold. The resulting micro-structured elastomer is peeled off by hand. The sealing of the PDMS microfluidic structure to the glass substrate (backside of the sensing part) is performed by activation of the glass and PDMS surfaces by oxygen plasma. This plasma treatment is performed with an OXFORD RIE machine and the following parameters: oxygen flow (20 sccm), power (75 W), pressure (150 mTorr), and time (15 s). This treatment makes the PDMS surface hydrophilic and allows bonding of both surfaces. The fluidic connections

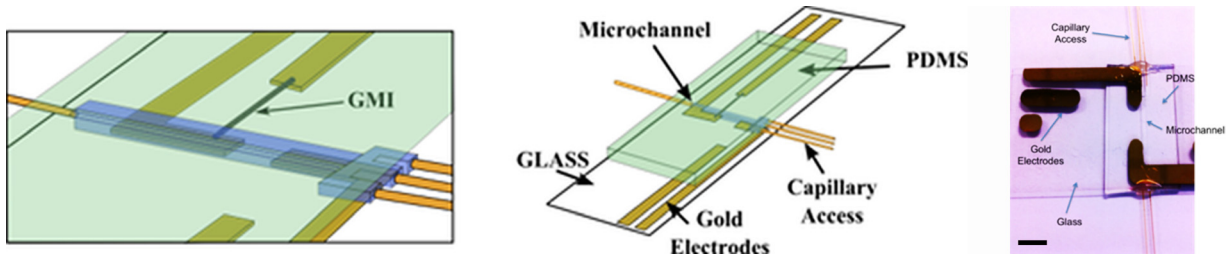

FIG. 2. Left to right 3D schematics of the microfluidic system showing the PDMS micro-channel on one side of the glass substrate and the GMI micro-wire and electrical connections on the other side, picture of the actual device (scale bar is 5 mm).

are obtained by bonding of fused silica capillaries laterally introduced in the PDMS channels and fixed by Araldite glue. Figure 2 represents 3D schematics of the resulting device and a picture of the actual device, respectively.

The experimental setup consists of two sets of Helmholtz coils to magnetize the USPIOs and to polarize the GMI magnetometer, respectively. The principle of the detection system has been described elsewhere.[48] The whole system is placed into a shielded box having a residual magnetic induction of around 0.13 μT (Fig. 3).

A liquid-liquid segmented multiphase flow is generated in the channel using a Y-shaped inlet junction and three programmable syringe-pumps (NE 1000 - New Era Pump Systems, Inc.).[51] Its pattern is characterized by dispersed phase plugs (water-based with the USPIOs) with equivalent diameter larger than the channel diameter that flow along the channel separated by the continuous phase oil-based plugs (Fig. 4). The size of the plug depends on many parameters of which the flow rates applied to the three inlets (from 0.5 mm to several mm). For instance, when we apply 0.9 μl/mn for the oil phase and 0.8 μl/mn for the water phase, we generate plugs 70 μm wide and 2 mm long (volume ~20 nl). A video camera (DigiMicro 2.0, 2 MegaPixel, ×20–×200) records the displacement of the USPIOs plugs. The amplitude and excitation frequency of the GMI magnetometer are 8 mT and 1.9 kHz, respectively. The signal to noise ratio (SNR) is 1.6 for a bandwidth of 7.8 Hz when the GMI wire is perpendicular to the micro-channel.

According to our theoretical modeling,[49] and considering the geometry of the microfluidic device used, the minimum amount of USPIOs that can be detected is around 4×10^{-9} mol, which corresponds to almost 20 nl plugs of USPIOs with molar concentration of 230 mmol/l. This is confirmed by the experiment (Fig. 5), where mono-phase (oil) flow (from 0 to 87 s.) induces only magnetic noise in the magnetometer while two-phase flow with the USPIOs (2 mm long, i.e.: 23.8 nl) generates magnetic field variations detected by the GMI sensor. One can observe that the signal increases when a plug approaches the GMI wire and decreases when it moves away, explaining its periodic variation. The detection of 5.47 nmol USPIOs plugs (2 mm × 70 μm × 170 μm, 230 mmol/l) is experimentally demonstrated.

Blood velocity is about 20 cm/s (i.e.: volumetric flow rate of 1.9 ml/s) in a small vein (i.e.: 3.5 mm diameter).[52,53] For safety reason, the molar concentration of USPIOs in the human body cannot exceed 40 μmol/l.[54] At a flow rate of 1.9 ml/s, it corresponds to 76×10^{-9} mol/s of USPIOs, which can be captured by high magnetic field gradients as in Refs. 55 and 56. Magnetic capture during 72 ms would form samples with USPIOs amount above the experimentally demonstrated detection level of our system (5.47×10^{-9} mol). Capturing particles over a longer period of time would further increase the amount of particles and consequently improve the SNR for the *ex-vivo* detection and subsequent analyses. It would be useful to introduce a microfluidic concentrator in front of the GMI detector to reduce the size of

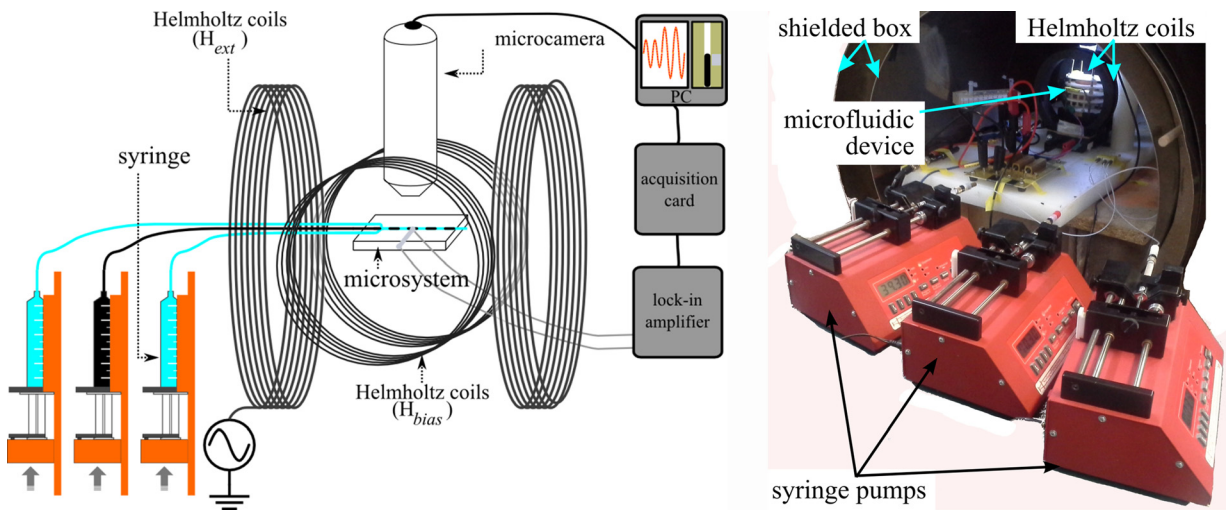

FIG. 3. Picture of the experimental bench where one can see the programmable syringe pumps, the shielded box, the Helmholtz coils, and the microfluidic system.

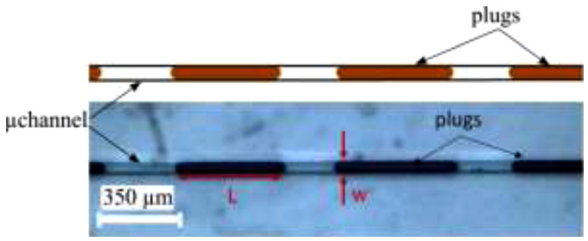

FIG. 4. Picture extracted from video showing plugs of 6 nl in the microchannel, with W = 70 μm (cross section 70 × 170 μm^2) and L = 490 μm.

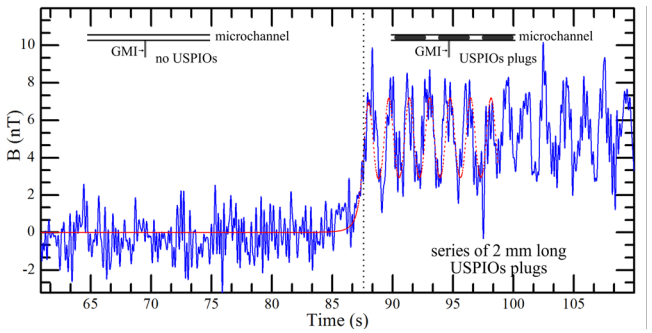

FIG. 5. Measured magnetic signal before and after (black dotted, t = 87.5 s) injection of the USPIOs plugs with 5.47×10^{-9} mol contents (2 mm long-20 nl volume with a molar concentration of 230 mmol/l). The dotted red curve is obtained from simulation with the model detailed in Ref. 49.

the plug as reported by Lin,[57] Zborowski,[58] or Wang.[59] In summary, this work is a first step toward a proof of concept of the feasibility to use USPIOs as CAs for in-vivo MRI and as biomolecules tags for *ex-vivo* bio-fluids analyses with lab-on-chip technology.

This work was partially supported by the French RENATECH network, the CNANO-NO Nanotrans program and the region Basse-Normandy.

[1]S. S. Kelkar and T. M. Reineke, "Theranostics: Combining imaging and therapy," Bioconjugate Chem. **22**, 1879–1903 (2011).
[2]J. T. Cole and N. B. Holland, "Multifunctional nanoparticles for use in theranostic applications," Drug Delivery Transl. Res. **5**, 295–309 (2015).
[3]J. L. Xie, G. Liu, H. S. Eden, H. Ai, and X. Chen, "Surface-engineered magnetic nanoparticle platforms for cancer imaging and therapy," Acc. Chem. Res. **44**, 883–892 (2011).
[4]D. C. Baiu, C. S. Brazel, Y. P. Bao, and M. Otto, "Interactions of iron oxide nanoparticles with the immune system: Challenges and opportunities for their use in nano-oncology," Curr. Pharm. Des. **19**, 6606–6621 (2013).
[5]J. Lodhia, G. Mandarano, N. J. Ferris, P. Eu, and S. F. Cowell, "Development and use of iron oxide nanoparticles (part 1): Synthesis of iron oxide nanoparticles for MRI," Biomed. Imaging Intervention J. **6**, e12 (2010).
[6]W. Wu, Z. Wu, T. Yu, C. Jiang, and W.-S. Kim, "Recent progress on magnetic iron oxide nanoparticles: Synthesis, surface functional strategies and biomedical applications," Sci. Technol. Adv. Mater. **16**, 023501 (2015).
[7]Q. A. Pankhurst, N. T. K. Thanh, S. K. Jones, and J. Dobson, "Progress in applications of magnetic nanoparticles in biomedicine," J. Phys. D: Appl. Phys. **42**, 224001 (2009).
[8]A. M. Dias, A. Hussain, A. S. Marcos, and A. C. Roque, "A biotechnological perspective on the application of iron oxide magnetic colloids modified with polysaccharides," Biotechnol. Adv. **29**, 142–155 (2011).
[9]D. L. Thorekm and A. Tsourkas, "Charge and concentration dependent uptake of iron oxide particles by non-phagocytic cells," Biomaterials **29**, 3583–3590 (2008).
[10]S. H. Bakhru, E. Altiok, C. Highley, D. Delubac, J. Suhan, T. K. Hitchens, C. Ho, and S. Zappe, "Enhanced cellular uptake and long-term retention of chitosan-modified iron-oxide nanoparticles for MRI-based cell tracking," Int. J. Nanomed. **7**, 4613–4623 (2012).
[11]M. C. Wang, L. D. Papsidero, M. Kuriyama, L. A. Valenzuela, G. P. Murphy, and T. M. Chu, "Prostate antigen: A new potential marker for prostatic cancer," Prostate **2**, 89–96 (1981).
[12]J. Mair, F. Dienstl, and B. Puschendorf, "Cardiac troponin T in the diagnosis of myocardial injury," Crit. Rev. Clin. Lab. Sci. **29**, 31–57 (1992).
[13]D. J. Brennan, D. P. O'Connor, E. Rexhepaj, F. Ponten, and W. M. Gallagher, "Antibody-based proteomics: Fast-tracking molecular diagnostics in oncology," Nat. Rev. Cancer **10**, 605–617 (2010).
[14]I. Georgakoudi, N. Solban, J. Novak, W. L. Rice, X. Wei, T. Hasan, and C. P. Lin, "*In vivo* flow cytometry: A new method for enumerating circulating cancer cells," Cancer Res. **64**, 5044–5047 (2004).
[15]E. I. Galanzha and V. P. Zharov, "Circulating tumor cell detection and capture by photoacoustic flow cytometry *in vivo* and *ex vivo*," Cancers **5**, 1691–1738 (2013).
[16]N. Saucedo-Zeni, S. Mewes, R. Niestroj, L. Gasiorowski, D. Murawa, and P. Nowaczyk, "Novel method for the *in vivo* isolation of circulating tumor cells from peripheral blood of cancer patients using a functionalized and structured medical wire," Int. J. Oncol. **41**, 1241–1250 (2012).
[17]H. Wang, G. F. Yue, C. Q. Dong, F. L. Wu, J. Wei, Y. Yang, Z. Zou, L. Wang, X. Qian, T. Zhang, and B. Liu, "Carboxybetaine methacrylate-modified nylon surface for circulating tumor cell capture," Appl. Mater. Interfaces **6**, 4550–4559 (2014).
[18]H. Zhang, Z. Jia, C. Wu, L. Zang, G. Yang, Z. Chen, and B. Tang, "*In vivo* capture of circulating tumor cells based on transfusion with a vein indwelling needle," Appl. Mater. Interfaces **7**, 20477−20484 (2015).
[19]N. Pamme, "Magnetism and microfluidics," Lab Chip **6**, 24–38 (2006).
[20]A. van Reenen, A. M. de Jong, J. M. J. den Toonder, and M. W. J. Prins, "Integrated lab-on-chip biosensing systems based on magnetic particle actuation – A comprehensive review," Lab Chip **14**, 1966–1986 (2014).
[21]B. D. Plouffe, S. K. Murthy, and L. H. Lewis, "Fundamentals and application of magnetic particles in cell isolation and enrichment: A review," Rep. Prog. Phys. **78**, 016601 (2015).
[22]R. L. Edelstein, C. R. Tamanaha, P. E. Sheehan, M. M. Miller, D. R. Baselt, L. J. Whitman, and R. J. Colton, "The BARC biosensor applied to the detection of biological warfare agents," Biosens. Bioelectron. **14**, 805–813 (2000).
[23]D. J. B. Bechstein, E. Ng, J. R. Lee, S. G. Cone, R. S. Gaster, S. J. Osterfeld, D. A. Hall, J. A. Weaver, R. J. Wilson, and S. X. Wang, "Microfluidic multiplexed partitioning enables flexible and effective utilization of magnetic sensor arrays," Lab Chip **15**, 4273–4276 (2015).
[24]G. G. Lin, D. Makarov, M. Medina-Sanchez, M. Guix, L. Baraban, G. Cuniberti, and O. G. Schmidt, "Magnetofluidic platform for multidimensional magnetic and optical barcoding of droplets," Lab Chip **15**, 216–224 (2015).
[25]G. Li, V. Joshi, R. L. White, S. X. Wang, J. T. Kemp, C. Webb, R. W. Davis, and S. Sun, "Detection of single micron-sized magnetic bead and magnetic nanoparticles using spin valve sensors for biological applications," J. Appl. Phys. **93**, 7557 (2003).
[26]H. A. Ferreira, N. Feliciano, D. L. Graham, and P. P. Freitas, "Effect of spin-valve sensor magnetostatic fields on nanobead detection for biochip applications," J. Appl. Phys. **97**, 10Q904 (2005).
[27]J. Devkota, G. Kokkinis, T. Berris, M. Jamalieh, S. Cardoso, F. Cardoso, H. Srikanth, M. H. Phan, and I. Giouroudi, "A novel approach for detection and quantification of magnetic nanomarkers using a spin valve GMR integrated microfluidic sensor," RSC Adv. **5**, 51169 (2015).
[28]F. Ludwig, S. Mäuselein, E. Heim, and M. Schilling, "Magnetorelaxometry of magnetic nanoparticles in magnetically unshielded environment utilizing a differential fluxgate arrangement," Rev. Sci. Instrum. **76**, 106102 (2005).
[29]Z. Yang, J. Lei, X. C. Sun, C. Lei, Y. Zhou, and Y. Liu, "A dynabeads-labeled immunoassay based on a fluxgate biosensor for the detection of biomarkers," Anal. Methods **7**, 2391–2398 (2015).
[30]F. Ludwig, E. Heim, S. Mäuselein, D. Eberbeck, and M. Schilling, "Magnetorelaxometry of magnetic nanoparticles with fluxgate magnetometers for the analysis of biological targets," J. Magn. Magn. Mater. **293**, 690–695 (2005).
[31]L. Ejsing, M. F. Hansen, and A. Menon, "Magnetic microbead detection using the planar Hall effect," J. Magn. Magn. Mater. **293**, 677–684 (2005).
[32]D. Issadore, J. Chung, H. Shao, M. Liong, A. A. Ghazani, C. M. Castro, R. Weissleder, and H. Lee, "Ultrasensitive clinical enumeration of rare cells *ex vivo* using a micro-hall detector," Sci. Transl. Med. **4**, 141ra92 (2012).
[33]D. Issadore, H. J. Chung, J. Chung, G. Budin, R. Weissleder, and H. Lee, "Ultrasensitive clinical enumeration of rare cells *ex vivo* using a micro-hall detector," Adv. Healthcare Mater. **2**, 1224–1228 (2013).

[34]G. V. Kurlyandskaya, M. L. Sanchez, B. Hernando, V. M. Prida, P. Gorria, and M. Tejedor, "Giant-magneto-impedance-based sensitive element as a model for biosensors," Appl. Phys. Lett. **82**, 3053 (2003).
[35]H. Chiriac, M. Tibu, A.-E. Moga, and D. D. Herea, "Magnetic GMI sensor for detection of biomolecules," J. Magn. Magn. Mater. **293**, 671–676 (2005).
[36]H. Yang, L. Chen, C. Lei, J. Zhang, D. Li, Z. Zhou, C. Bao, H. Hu, X. Chen, F. Cui, S. Zhang, Y. Zhou, and D. Cui, "Giant magnetoimpedance-based microchannel system for quick and parallel genotyping of human papilloma virus type 16/18," Appl. Phys. Lett. **97**, 043702 (2010).
[37]D. Karnaushenko, D. D. Karnaushenko, D. Makarov, S. Baunack, R. Schafer, and O. G. Schmidt, "Self-assembled on-chip-integrated giant magneto-impedance sensorics," Adv. Mater. **27**, 6582–6589 (2015).
[38]B. Dufay, S. Saez, C. Dolabdjian, A. Yelon, and D. Menard, "Physical properties and giant magnetoimpedance sensitivity of rapidly solidified magnetic microwires," J. Magn. Magn. Mater. **324**, 2091–2099 (2012).
[39]E. Fernandes, V. C. Martins, C. Nóbrega, C. M. Carvalho, F. A. Cardoso, S. Cardoso, J. Dias, D. Deng, L. D. Kluskens, and P. P. Freitas, "A bacteriophage detection tool for viability assessment of Salmonella cells," Biosens. Bioelectron. **52**, 239–246 (2014).
[40]N. Pekas, M. D. Porter, M. Tondra, A. Popple, and A. Jander, "Giant magnetoresistance monitoring of magnetic pico-droplets in an integrated microfluidic system," Appl. Phys. Lett. **85**, 4783–4785 (2004).
[41]L. Lagae, R. Wirix-Speetjens, J. Das, D. Graham, H. Ferreira, P. P. F. Freitas, G. Borghs, and J. De Boeck, "On-chip manipulation and magnetization assessment of magnetic bead ensembles by integrated spin-valve sensors," J. Appl. Phys. **91**, 7445–7447 (2002).
[42]J. Loureiro, R. Ferreira, S. Cardoso, P. P. Freitas, J. Germano, C. Fermon, G. Arrias, M. Pannetier-Lecoeur, F. Rivadulla, and J. Rivas, "Toward a magnetoresistive chip cytometer: Integrated detection of magnetic beads flowing at cm/s velocities in microfluidic channels," Appl. Phys. Lett. **95**, 034104 (2009).
[43]J. Loureiro, P. Z. Andrade, S. Cardoso, C. L. da Silva, J. M. Cabral, and P. P. Freitas, "Magnetoresistive chip cytometer," Lab Chip **11**, 2255–2261 (2011).
[44]M. Helou, M. Reisbeck, S. F. Tedde, L. Richter, L. Bär, J. J. Bosch, R. H. Stauber, E. Quandt, and O. Hayden, "Time-of-flight magnetic flow cytometry in whole blood with integrated sample preparation," Lab Chip **13**, 1035–1038 (2013).
[45]A. Vila, V. C. Martins, A. Chícharo, C. Rodriguez-Abreu, A. C. Fernandes, F. A. Cardoso, S. Cardoso, J. Rivas, and P. Freitas, "Customized design of magnetic beads for dynamic magnetoresistive cytometry," IEEE Trans. Magn. **50**, 5101904 (2014).
[46]A. C. Fernandes, C. M. Duarte, F. A. Cardoso, R. Bexiga, S. Cardoso, and P. P. Freitas, "Lab-on-chip cytometry based on magnetoresistive sensors for bacteria detection in milk," Sensors **14**, 15496–15523 (2014).
[47]A. Garcia-Arribas, F. Martinez, E. Fernandez, I. Ozaeta, G. V. Kurlyandskaya, A. V. Svalov, J. Berganzo, and J. M. Barandiaran, "GMI detection of magnetic-particles concentration in continuous flow," Sens. Actuators, A **172**, 103–108 (2011).
[48]K. Fodil, M. Denoual, C. Dolabdjian, M. Harnois, and V. Senez, "Dynamic sensing of magnetic nanoparticles in microchannel using GMI technology," IEEE Trans. Magn. **49**, 93–96 (2013).
[49]K. Fodil, M. Denoual, C. Dolabdjian, A. Treizebre, and V. Senez, "Model calculation of the magnetic induction generated by the magnetic nanoparticles flowing into a microfluidic system: Performance analysis of the detection," IEEE Trans. Magn. **50**, 5300108 (2014).
[50]P. P. Freitas and H. A. Ferreira, "Spintronic biochips for biomolecular recognition," in *Handbook of Magnetism and Advanced Magnetic Materials* (Wiley, 2007), pp. 1–29.
[51]A. L. Dessimoz, L. Cavin, A. Renken, and L. Kiwi-Minsker, "Liquid-liquid two-phase flow patterns and mass transfer characteristics in rectangular glass microreactors," Chem. Eng. Sci. **63**, 4035–4044 (2008).
[52]M. P. Wiedeman, "Dimensions of blood vessels from distributing artery to collecting vein," Circ. Res. **12**, 375–378 (1963).
[53]A. S. Popel and P. C. Johnson, "Microcirculation and hemorheology," Annu. Rev. Fluid Mech. **37**, 43–69 (2005).
[54]V. Dousset, C. Gomez, K. G. Petry, C. Delalande, and J. M. Caille, "Dose and scanning delay using USPIO for central nervous system macrophage imaging," Magn. Reson. Mater. Phys., Biol. Med. **8**, 185–189 (1999).
[55]N. Xia, T. P. Hunt, B. T. Payers, E. Alsberg, G. M. Whitesides, R. M. Westervelt, and D. E. Ingber, "Combined microfluidic-micromagnetic separation of living cells in continuous flow," Biomed. Microdevices **8**, 299–308 (2009).
[56]R. M. Cooper, D. C. Leslie, K. Domansky, A. Jain, C. Yung, M. Cho, S. Workam, M. Super, and D. E. Ingber, "A microdevice for rapid optical detection of magnetically captured rare blood pathogens," Lab Chip **14**, 182–188 (2014).
[57]J. H. Lin, M. Li, Y. B. Li, Q. Chen, and J. M. Caille, "A high gradient and strength bioseparator with nano-sized immunomagnetic particles for specific separation and efficient concentration of *E-coli* O157:H7," J. Magn. Magn. Mater. **378**, 206–213 (2015).
[58]P. S. Williams, F. Carpino, and M. Zborowski, "Characterization of magnetic nanoparticles using programmed quadrupole magnetic field-flow fractionation," Philos. Trans. R. Soc., A **368**, 4419–4437 (2010).
[59]C. M. Earhart, C. E. Hughes, R. S. Gaster, C. C. Ooi, R. J. Wilson, L. Y. Zhou, E. W. Humke, L. Xu, D. J. Wong, S. B. Willingham, E. J. Schwartz, I. L. Weissman, S. S. Jeffrey, J. W. Neal, R. Rohatgi, H. A. Wakelee, and S. X. Wang, "Isolation and mutational analysis of circulating tumor cells from lung cancer patients with magnetic sifters and biochips," Lab Chip **14**, 78–88 (2014).